

Downlink Joint Rate and Power Allocation in Cellular Multirate WCDMA Systems

Dong In Kim, *Senior Member, IEEE*, Ekram Hossain, *Member, IEEE*, and Vijay K. Bhargava, *Fellow, IEEE*

Abstract—This paper proposes a novel dynamic joint rate and power control procedure for downlink data transmission in a multicell variable spreading factor wideband code-division multiple-access (WCDMA) system where the different users have similar quality-of-service requirements in terms of the signal-to-interference ratio (SIR). Two variations of the dynamic joint rate and power allocation procedure, namely, *Algorithm-1* and *Algorithm-2*, are presented. The performances of these two schemes are compared to the performance of the *optimal* dynamic link adaptation for which the rate and power allocation is found by an exhaustive search. The optimality criterion is the maximization of the total radio link level capacity (or sum-rate capacity) in terms of the average number of radio link level frame transmitted per adaptation interval under constrained SIR and power limit in the base station transmitter. The proposed schemes have linear time complexity as compared to the exponential time complexity of the optimal scheme and achieve better radio link level throughput fairness compared to the optimal link adaptation scheme with a moderate loss in total throughput. Performance evaluation is carried out under random and directional micromobility models with uncorrelated and correlated long-term fading, respectively, in a cellular WCDMA environment for both the homogeneous (or uniform) and the nonhomogeneous (or nonuniform) traffic load scenarios.

Index Terms—Dynamic rate and power adaptation, multicell multirate wideband code-division multiple-access (WCDMA) systems, radio link level throughput fairness.

I. INTRODUCTION

THIRD-GENERATION (3-G) **<Author: Please define “PP”>** PP wideband code-division multiple-access (WCDMA) system, which is being developed as one of the IMT-2000 standards, is expected to provide high-speed packet data services with different quality-of-service (QoS) support for 3-G wireless communications. In a WCDMA system, the transmission rate and the power corresponding to the different mobile users can be dynamically varied depending on the variations of the channel condition to improve the spectral efficiency while meeting the QoS requirements of the mobile

Manuscript received February 8, 2001; revised August 18, 2001, March 9, 2002, and April 5, 2002; accepted April 8, 2002. The editor coordinating the review of this paper and approving it for publication is S. Roy. This work was supported in part by the Brain Korea 21 Project in 2000 and in part by a Strategic Project Grant from the Natural Sciences and Engineering Research Council (NSERC) of Canada.

D. I. Kim is with the Department of Electrical and Computer Engineering, University of Seoul, Seoul, Korea 130-743 (e-mail: dikim@uoscc.uos.ac.kr).

E. Hossain is with the Department of Electrical and Computer Engineering, University of Manitoba, Winnipeg, MB, Canada R3T 5V6 (e-mail: ekram@ee.umanitoba.ca).

V. K. Bhargava is with the Department of Electrical and Computer Engineering, University of Victoria, Victoria, BC, Canada V8W 3P6 (e-mail: bhargava@ece.uvic.ca).

Digital Object Identifier 10.1109/TWC.2002.806366

users. The data transmission rate in the forward link physical layer of a WCDMA system can be controlled by using the variable spreading factor (VSF) method or the multicode method [1]. This paper proposes a novel joint adaptive rate and power adaptation procedure for downlink data transmission in multicell VSF WCDMA systems where the mobile data users are assumed to have similar signal-to-interference ratio (SIR) [and hence similar bit-error rate (BER)] requirements.

In an interference-limited environment, channel utilization (and hence the system capacity) can be enhanced by suitable rate and power allocation to the mobiles based on the corresponding interference and fading conditions—if a mobile experiences larger interference, the rate assignment for this mobile is to be constrained to lower rates compared to that for the mobile with better channel conditions. This is similar to the dynamic link adaptation concept proposed for narrowband systems [2]. In this paper, a joint dynamic rate and power adaptation procedure is proposed (with two variations) for both uniform and nonuniform traffic loads in a multicell environment considering both *random mobility with uncorrelated shadowing* and *directional mobility with correlated shadowing*. Since the short-term fading (i.e., multipath fading) changes more rapidly compared to the long-term fading (i.e., path loss and shadowing), multipath fading is assumed to be independent.

The organization of the rest of the paper is as follows. Section II presents the background and motivation of the work. In Section III, a model is developed to evaluate the SIR and based upon it the optimal rate and power allocation is determined for downlink data transmission in a multicell VSF WCDMA system. In Section IV, two suboptimal joint rate and power allocation algorithms, namely, *Algorithm-1* and *Algorithm-2*, are presented for dynamically adjusting the transmission rate and the transmission power corresponding to the different mobiles. In Section V, the sum-rate capacity is investigated analytically for joint rate and power adaptation using *Algorithm-2*. The simulation model along with the simulation, the seminumerical and the analytical results are presented in Section VI. In Section VII, conclusions are stated.

II. BACKGROUND AND MOTIVATION

The problem of optimal rate and power adaptation for *uplink* packet data transmission in a *single-cell multirate* CDMA system was addressed in [3] and the optimal centralized adaptive rate and power control strategy to maximize the total average weighted throughput was determined. With the objective of maximizing the throughput and with the constraints on maximum power and/or minimum rate, the problem of jointly controlling the user power and data rates for *uplink* data

transmission in a *single-cell* CDMA system was formulated as a constrained optimization problem in [4]–[6]. In [7], the throughput maximization problem for CDMA *uplinks* was formulated as an optimization problem in terms of the spreading gains and the transmit powers of the users.

However, the problem of joint rate and power adaptation under constrained SIR and power limit for *downlink* data transmission in a *multicell* and *multirate* CDMA system has not been studied. In this paper, we address this problem and based upon a simplified SIR model for downlink data transmission in a multicell VSF WCDMA system, we find out the *optimal* solution by an exhaustive search in the solution space. The optimality criterion here is the maximization of the total radio link level capacity (or sum-rate capacity) in terms of the average number of radio link level frame transmitted per adaptation interval under constrained SIR and power limit in the base station (BS) transmitter. The spatial distribution of the users along with the short-term and long-term channel fading are explicitly taken into account. Since in a cellular WCDMA system with large number of users, implementation of such an optimal scheme would be infeasible due to the huge computational complexity, we propose two very simple (implementation-friendly) suboptimal schemes. The sum-rate capacity of these suboptimal schemes are compared to the optimal scheme.

Again, most of the recent papers [7]–[11] reveal that the throughput-maximizing rate allocation with power limit permits only very few users (with favorable channel conditions) to transmit at or near the maximum allowable rate, and the rest of the users do not transmit at all. This implies that the throughput-maximizing rate distributions are extreme, which may cause unfairness in radio link level [and hence higher layer protocol, e.g., transmission control protocol (TCP)] throughput performance in a cell. In the same way, the above optimal rate and power allocation is likely to cause the fairness problem among cells, as well as users in a cell. Therefore, the performances of the suboptimal schemes are compared with the performance of the optimal scheme in view of both the sum-rate capacity and the fairness.

The simplistic SIR model along with the simple dynamic rate and power allocation schemes would enable us to evaluate the higher layer protocol performance under dynamic link adaptation and understand the interlayer protocol interactions in multirate cellular WCDMA networks.

III. MODELING OF DOWNLINK SIR AND OPTIMAL RATE AND POWER ALLOCATION

A. Modeling of Downlink SIR

We consider a variable rate downlink data transmission system for WCDMA-based cellular networks where the transmission rates can be selected from the set of rates $\{v_0, v_1, \dots, v_\varphi\}$. If it is assumed that $v_m = mv_1$ ($m = 0, 1, \dots, \varphi$)¹, and that only one frame (of fixed length of M bits) corresponding to the basic rate v_1 can be transmitted during a frame time, then for transmission rate

¹For the rest of the paper, it is assumed that $v_m = mv_1$ so that the normalized value of v_m with respect to the basic rate v_1 is m .

TABLE I
LIST OF KEY NOTATIONS

Parameter	Value
Frame-time, T	10 <i>ms</i>
Chip sequence length, N	128
Path loss exponent, δ	4.0
Standard dev. of shadow fading, σ	8 <i>dB</i>
ν	0.2
P_c/P_B	0.05, 0.1, 0.2
D	100 <i>m</i>
ε_D	0.1
A_θ	4.2
v	20, 50, 80 <i>km/hr</i>
φ	8
J	2, 18

of v_m , m frames can be transmitted during the same time. For this, a VSF WCDMA system can be used where the basic gain is given by N chips per bit, and in the case of rate v_m , the spreading gain is reduced to N/m chips per bit.

Table I lists notations on key parameters to be used in the downlink SIR modeling below.

Suppose that $P_{b,i}^{(j)}$ is the transmission power corresponding to the i th mobile station (MS) in cell j when the basic rate v_1 is used for transmission to the MS in the downlink. Then, in order to achieve the same BER performance, the power allocation for rate v_m would be $mP_{b,i}^{(j)}$.

Now assume that the number of MSs in cell j is g_j ($j = 0, 1, \dots, J$), and that the MSs in a cell are uniformly distributed. The radio propagation is modeled by path loss, shadowing and multipath fading. The signal from the base station j' (denoted by (BS) _{j'}) to the i th mobile of cell j (tagged cell) is attenuated by the δ th power of the distance and log-normal shadowing, that is, the signal power received at the i th mobile in cell j from (BS) _{j'} is

$$L_{j'}(j, i) = r_{i,j'}^{-\delta} \cdot 10^{\xi_{i,j'}/10}. \quad (1)$$

The signal is also affected by an L -path Rayleigh fading with path gain $a_{i,j',l}$ ($l = 1, 2, \dots, L$), where $\sum_{l=1}^L a_{i,j',l}^2 \triangleq \zeta_i^{(j')}$.

CDMA systems are generally interference-dominant and if noise becomes dominant, the capacity of such a system cannot be fully utilized. Near the capacity limit, time-division multiple-access systems are interference-limited too (due to co-channel interference). Since we are concerned with the maximum sum-rate capacity, we are considering a system which should operate near its maximum capacity. In fact, the optimal rate allocation scheme induces the sum-rate capacity to the maximum transmission rate supportable in each power-constrained cell. For this reason, the noise term is ignored in the modeling and analysis of downlink SIR below.

The output signal-to-interference ratio (SIR) _{o,i,l} ^(j) for the l th path, at the i th mobile of cell j can be expressed as in (2), shown at the bottom of the next page, where $\nu \leq 1$ represents the *orthogonality factor* in downlink ($\nu = 1$ corresponds to perfectly orthogonal in-cell mobiles) to account for the self-interference due to delayed multipath components even

with in-cell synchronous transmission, while for intercell asynchronous transmission [12] $\nu = 0$, and $m_i^{(j)} \in \{0, 1, \dots, \varphi\}$ denotes the rate allocation to the i th mobile in cell j .

In fact, ν depends on the location of each MS in cell j and also the characteristics of the multipath fading channel. For simplicity, in the SIR model developed below the effects of user location and multipath fading on ν are not taken into account and a constant value (< 1) of ν is assumed.

If we include the transmission power of any of the control channels (e.g., pilot channel) in (2), the RAKE-combined output $(\text{SIR})_{o,i}^{(j)} = \sum_{l=1}^L (\text{SIR})_{o,i,l}^{(j)}$ can be effectively modeled as in (3), shown at the bottom of the page, where P_c indicates the pilot-signal transmission power and $\eta_{j'/j}(i)$ is the *intercell interference factor* defined as follows:

$$\eta_{j'/j}(i) \triangleq \frac{\zeta_i^{(j')} L_{j'}(j, i)}{\zeta_i^{(j)} L_j(j, i)}. \quad (4)$$

Let us denote $P_{B,j}$ as the total transmission power at the $(\text{BS})_j$, namely,

$$P_{B,j} = \sum_{k=1}^{g_j} m_k^{(j)} P_{b,k}^{(j)} + P_c. \quad (5)$$

Then, the RAKE-combined output $(\text{SIR})_{o,i}^{(j)}$ at the i th MS of cell j can be expressed by

$$(\text{SIR})_{o,i}^{(j)} = \frac{P_{b,i}^{(j)} N}{P_{B,j} \left[(1 - \nu) + \sum_{j' \neq j} \beta_{j'/j} \cdot \eta_{j'/j}(i) \right]} \quad (6)$$

where $\beta_{j'/j} = P_{B,j'}/P_{B,j}$.

B. Optimal Rate and Power Allocation

Based on the above SIR modeling, an optimal rate and power allocation is performed in the sense that the sum-rate capacity $\sum_{j=0}^J \sum_{i=1}^{g_j} m_i^{(j)}$ is maximized with the SIR and power constraints such as

$$(\text{SIR})_{o,i}^{(j)} = (\text{SIR})_{o,d} \geq (\text{SIR})_o \quad \forall i, j \quad (7)$$

$$\frac{1}{(J+1)} \sum_{j=0}^J P_{B,j} \leq P_B \quad (8)$$

where $(\text{SIR})_o = E_b/I_o$ is the target SIR and P_B is the average power constraint per cell (i.e., average power budget available at the BS of a cell). It is to be noted that the “rate 0” is allowed for the maximum sum-rate capacity (i.e., $m_i^{(j)} \in \{0, 1, \dots, \varphi\}$).

Proposition 1: To maintain the same downlink quality $(\text{SIR})_{o,i}^{(j)} = (\text{SIR})_{o,d}^{(j)}$ for all $i = 1, \dots, g_j$ in cell j , the RAKE-combined output SIR expression in (6) can be formulated as

$$(\text{SIR})_{o,d}^{(j)} = \frac{N}{\sum_{k=1}^{g_j} m_k^{(j)} \mu_k^{(j)}} \left(1 - \frac{P_c}{P_{B,j}} \right) \quad (9)$$

where the *effective interference factor* $\mu_k^{(j)}$ in cell j is given by

$$\mu_k^{(j)} = \left[(1 - \nu) + \sum_{j' \neq j} \beta_{j'/j} \cdot \eta_{j'/j}(k) \right]. \quad (10)$$

Proof of Proposition 1: First, in order to have the same downlink quality for all MSs in the tagged cell j , (6) should be of the form

$$(\text{SIR})_{o,i}^{(j)} = \frac{\rho_j N}{P_{B,j}}. \quad (11)$$

Here, the parameter ρ_j which is kept the same for all MSs in cell j , is defined by

$$\rho_j = \frac{P_{b,i}^{(j)}}{\mu_i^{(j)}}, \quad i = 1, \dots, g_j \quad (12)$$

where the effective interference factor $\mu_i^{(j)}$ in cell j is given by (10) with the index k replaced by i . We note that the effective interference in each mobile in cell j is modeled in terms of the in-cell orthogonality factor ν , the power ratio $\beta_{j'/j}$, and the intercell interference factor $\eta_{j'/j}(i)$ that also includes the multipath fading. The results in [13, eq. 21, p. 309] can be considered as special cases of the above formulation when $\nu = 0$, $\beta_{j'/j} = 1$, and $\zeta_i^{(j)} = 1$ (no fading).

Now, substituting $P_{b,k}^{(j)} = \rho_j \cdot \mu_k^{(j)}$ [from (12)] into (5) gives

$$\rho_j = \frac{P_{B,j} - P_c}{\sum_{k=1}^{g_j} m_k^{(j)} \mu_k^{(j)}} \quad (13)$$

and then combining this with (11) ends up with (3). ■

It is to be noted that the communication quality will fluctuate across the cells unless $\{P_{B,j} \mid j = 0, 1, \dots, J\}$ are properly

$$(\text{SIR})_{o,i,l}^{(j)} = \frac{a_{i,j,l}^2 \left(m_i^{(j)} P_{b,i}^{(j)} \right) \left(\frac{N}{m_i^{(j)}} \right) L_j(j, i)}{\sum_{k=1}^{g_j} m_k^{(j)} P_{b,k}^{(j)} \zeta_i^{(j)} (1 - \nu) L_j(j, i) + \sum_{j' \neq j} \sum_{k=1}^{g_{j'}} m_k^{(j')} P_{b,k}^{(j')} \zeta_i^{(j')} L_{j'}(j, i)} \quad (2)$$

$$(\text{SIR})_{o,i}^{(j)} = \frac{P_{b,i}^{(j)} N}{(1 - \nu) \left(\sum_{k=1}^{g_j} m_k^{(j)} P_{b,k}^{(j)} + P_c \right) + \sum_{j' \neq j} \left(\sum_{k=1}^{g_{j'}} m_k^{(j')} P_{b,k}^{(j')} + P_c \right) \cdot \eta_{j'/j}(i)} \quad (3)$$

allocated to yield $(\text{SIR})_{o,d}^{(j)} = (\text{SIR})_{o,d}$ for all j . For this reason, it is required to globally allocate $\{P_{B,j}\}$ such that the downlink quality for all cells is kept the same.

From (9) and (10), if we let $(\text{SIR})_{o,d}^{(j)} = (\text{SIR})_{o,d}$ for all j along with $\beta_{j'}/j = P_{B,j'}/P_{B,j}$, we obtain $(J+1)$ simultaneous linear equations in (14)

$$\beta_j \left[N - (1 - \nu) \sum_{k=1}^{g_j} m_k^{(j)} (\text{SIR})_{o,d} \right] - \sum_{k=1}^{g_j} m_k^{(j)} \sum_{j' \neq j} \beta_{j'} \cdot \eta_{j'/j}(k) \cdot (\text{SIR})_{o,d} = N, \quad j = 0, 1, \dots, J \quad (14)$$

where $\beta_j = P_{B,j}/P_c$.

In general, given $\{g_j\}$, $\{m_k^{(j)}\}$ and $\{\eta_{j'/j}(k)\}$ along with N and ν , these equations can be solved so as to yield the global power allocations $\{P_{B,j} \mid j = 0, 1, \dots, J\}$ with the constraints $(\text{SIR})_{o,d} \geq (\text{SIR})_o$ and $1/(J+1) \sum_{j=0}^J \beta_j \leq P_B/P_c$. Once the per-cell power allocations $\{P_{B,j}\}$ are determined by (14), the per-user power allocation at basic rate $\{P_{b,i}^{(j)}\}$ can be found using (10), (11), and (12) with the constraint $(\text{SIR})_{o,i}^{(j)} \geq (\text{SIR})_o$.

Using (14), the optimal rate and power allocation during each adaptation interval can be determined by an exhaustive search for the rate combinations $\{m_i^{(j)} \mid j = 0, 1, \dots, J; i = 1, \dots, g_j\}$ that maximizes the sum-rate capacity within the SIR and power constraints. It is to be noted that, inclusion of a constraint on throughput fairness (*over each adaptation interval*) among the users and across the cells in the general optimization approach above would make it computationally prohibitive. Again, ensuring fairness in a very small time-scale (e.g., one adaptation interval) would be impractical due to the highly degraded channel utilization. Therefore, the *fairness* among the different users is generally measured over several frame-periods (rather than over each frame period).

It is to be noted that, the above approach to optimal rate and power allocation considers common SIR requirement for all the mobiles in all the cells. The problem of dynamic rate and power adaptation under multiple SIR constraints (e.g., different SIR requirements for the different mobiles in the different cells) can be addressed under the above optimal rate and power allocation framework even though the computational complexity of adaptation would increase.

It is not difficult to observe that the computational complexity of the exhaustive search for determining the optimal rate and power allocation would be of $O(((\varphi+1)^{g_j})^{J+1}) \times O((J+1)^3)$. Since finding the optimal solution requires cycling through all possible assignments which would involve exponential time complexity, the problem of optimal rate selection (which is similar to the *satisfiability problem* ([14, p. 673])) is NP-complete. Therefore, it is unlikely that a true optimal algorithm for this problem (other than the exhaustive search) exists. Hence, in a practical scenario, a fast and efficient procedure would be desirable which may not necessarily result in true optimal rate and power allocation (from the viewpoint of total sum-rate capacity) but a suboptimal rate and power allocation.

Again, the optimal rate and power allocation is also likely to cause the fairness problem among users in different cells, as well as users in a cell. Therefore, we propose the two suboptimal dynamic rate and power allocation schemes which greatly reduce the computational complexity while increasing the fairness across the cells. The sum-rate capacity and the radio link level throughput fairness (among users in different cells) for these two schemes are compared with those of the optimal rate and power allocation scheme.

The rate allocations $\{m_i^{(j)}\}$ and the per-user power allocations at basic rate $\{P_{b,i}^{(j)}\}$ under the proposed suboptimal schemes are dependent on the interference distribution. The dynamic rate and per-user power (at basic rate) adaptation is made in such a way that higher transmission rates are assigned to mobiles experiencing lower interference, whereas lower powers assigned to the mobiles as given in (12) for fixed ρ_j . The per-cell power allocations $\{P_{B,j}\}$ for these suboptimal rate and power adaptation algorithms are heuristic-based and are determined by the traffic load distribution over the cells. The suboptimal schemes are expected to improve the throughput fairness with reasonably high sum-rate capacity.

IV. SUBOPTIMAL JOINT RATE AND POWER ALLOCATION

A. Uniform Traffic

With uniform traffic distribution, the traffic load is on the average same in all cells, and the same power constraint applies to all the cells, i.e., the power constraint is modified as $P_{B,j} \leq P_B \forall j$. The rationale behind this is that the optimal rate allocation will increase the sum-rate capacity to the maximum allowable rate in each cell. Then, the throughput fairness among users in different cells (or intercell throughput fairness) may be achieved by constraining the total transmission power at the BS to the same limit. In fact, the optimal algorithm searches for a user with least interference condition (level) across the $(J+1)$ cells involved to maximize the sum-rate capacity. Therefore, the rate allocation among users is expected to become more "nonuniform" compared to the suboptimal algorithms for which the search can be limited within a cell with the power allocations per-cell (i.e., $\{P_{B,j}\}$) heuristically determined.

We assume that the target $(\text{SIR})_o$ corresponding to some desired BER performance (e.g., $\text{BER} \leq 10^{-5}$) is known to the BS and that the traffic loads in all the cells are the same. Then, using (9) and since $P_{B,j} \leq P_B$, for a given traffic load of G per cell

$$\sum_{k=1}^G m_k^{(j)} \mu_k^{(j)} \leq \frac{N}{(\text{SIR})_o} \left(1 - \frac{P_c}{P_B}\right) \triangleq \gamma. \quad (15)$$

This bound enables us to jointly allocate the rate and the power to the mobiles when the corresponding effective interference factors $\{\mu_k^{(j)}\}_{k=1}^G$ are known.

Based on the measured/computed $\{\mu_k^{(j)}\}_{k=1}^G$, the rate $m_k^{(j)}$ ($k = 1, \dots, G$) is adaptively changed in such a way that the weighted *sum interference* (i.e., $\sum_{k=1}^G m_k^{(j)} \mu_k^{(j)}$) does not exceed γ , the *a priori* bound. Regarding the per-user power

allocation at basic rate, since the downlink quality should be maintained the same for all mobiles, it is obvious that

$$P_{b,k}^{(j)} = \rho_j \cdot \mu_k^{(j)}, \quad k = 1, \dots, G. \quad (16)$$

It is to be noted that, under uniform traffic case, even though the number of mobiles is the same in all the cells, the path gains and the interference conditions may not be necessarily same in all the cells. Therefore, the rate allocation among the mobiles in the different cells may not be the same if a snapshot is considered.

In the algorithms below, the MSs are assumed to be logically arranged in a list in the increasing order of the corresponding interference factors. Note that, for both the algorithms, the key parameter is $\mu_k^{(j)}$ which is to be measured or computed. This implementation issue will be discussed in Section IV-A4.

1) *Rate Allocation Algorithm-1*: The rate allocation is made such that the sum-rate capacity, namely, $\sum_{k=1}^G m_k^{(j)}$, is maximized while satisfying the constraint in (15). The rate allocation algorithm can be stated as follows:

(i) Initialize i to 1 and `weighted_sum_interference` to 0.0.
(ii) Allocate the maximum possible rate v_m ($m \leq \varphi$) to the i th MS with interference factor $\mu_i^{(j)}$ such that `weighted_sum_interference` + $m\mu_i^{(j)} \leq \gamma$ and update `weighted_sum_interference` to `weighted_sum_interference` + $m\mu_i^{(j)}$
(iii) Increment i and repeat step (ii) for the next candidate mobile (in the list).

In this case, rates are assigned to the mobiles in a “depth-first” fashion starting from the one experiencing the lowest interference. In this case, due to the “aggressive” rate allocation corresponding to connections with better channel conditions the radio link level sum-rate capacity is expected to be high. Since in this case the rate change can be “abrupt” from frame time to frame time, the variance of the radio link level frame transmission delay can be high.

2) *Rate Allocation Algorithm-2*: In this case, the rate corresponding to each mobile is first set to be inversely proportional to the corresponding interference factor. Then the rate allocations are updated in a “breadth-first” fashion as far as the sum interference is less than γ as in (15).

The algorithm can be expressed as follows:

(i). As long as the inequality in (15) is satisfied, allocate rates to all the mobiles according to $m_k^{(j)} = \min(\langle \alpha/\mu_k^{(j)} \rangle, \varphi)$ $k = 1, \dots, G$ where $\langle x \rangle$ is the integer nearest to x , $\alpha = N/G(1 - (P_c/P_B))$ $(SIR)_o^{-1}$ and $P_{B,j} = P_B$.
(ii). Update the rate allocation in a ‘breadth-first’ fashion over all the MSs such that the sum interference does not exceed γ .

This algorithm (as described inside the box below) makes the rate change from frame time to frame-time smoother (compared to *Algorithm-1*) so that a more uniform delay will be incurred at the radio link level. With dynamic link adaptation using *Algorithm-2*, the throughput fairness is expected to be higher compared to that for *Algorithm-1*.

3) *Power Allocation*: As for the per-user power allocation at basic rate, the parameter ρ_j in (16) is found as

$$\rho_j = \frac{P_B - P_c}{\sum_{k=1}^G m_k^{(j)} \mu_k^{(j)}}. \quad (17)$$

This can be interpreted as *joint* rate and power allocation because the power allocation itself depends on the rate allocation. Also, it is observed that the *effective total power* in traffic channel converges to

$$\sum_{k=1}^G m_k^{(j)} P_{b,k}^{(j)} \longrightarrow (\rho_j \alpha) G \quad (18)$$

for the rate allocation using *Algorithm-2*. In other words, the product of power (at basic rate) and rate per traffic channel is kept constant at $\rho_j \alpha$ regardless of the effective interference factor.

4) *Implementation Issue*: Given the target $(SIR)_o$ and the traffic load G , the parameter $\mu_k^{(j)}$ ($k = 1, \dots, G$) needs to be measured/computed periodically every adaptation interval. The effective interference factor $\mu_k^{(j)}$ can be measured using (10) assuming that the MS location can be tracked at the BS. A more practical way of implementation would be to compute the parameter by using the link quality estimates (e.g., $(SIR)_{o,k}^{(j)}$) at each mobile.

From (11) and (12), we obtain

$$\mu_k^{(j)} = \frac{N}{(SIR)_{o,k}^{(j)}} \frac{P_{b,k}^{(j)}}{P_B} \quad (19)$$

with $P_{B,j} = P_B$. Therefore, if each mobile continuously measures the link quality in terms of $(SIR)_{o,k}^{(j)}$ and reports any change in $(SIR)_{o,k}^{(j)}$ to the BS, then based on the values of $P_{b,k}^{(j)}$ and P_B , the effective interference factor $\mu_k^{(j)}$ for the next adaptation interval can be computed at the BS using (19) for a given processing gain N . After $\mu_k^{(j)}$ is computed, the rate allocations $(m_k^{(j)}, k = 1, 2, \dots, G)$ can be determined. Based on $\mu_k^{(j)}$ and $m_k^{(j)}$, the parameter ρ_j and hence the power allocations can be determined at the BSs. In this way, the above joint rate and power adaptation algorithms can be implemented in a *mobile-assisted and base-station controlled* manner. The implementation procedure is shown by a flow diagram in Fig. 1.

This SIR measurement-based rate allocation may not cause extra overhead since the mobile units may perform the SIR measurements (which would be required for power control purposes anyway) on a per-slot basis during each frame time which typically consists of 16 power control slots (or groups). The measured SIR values can be transmitted to the BS (e.g., through the uplink DPCCH in ETSI WCDMA [12]) periodically.

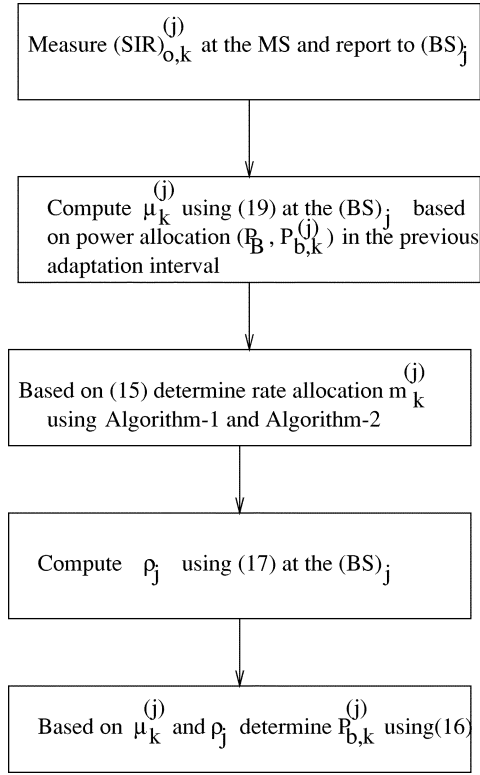


Fig. 1. Flow diagram for joint rate and power allocation in the case of uniform traffic.

B. Nonuniform Traffic

For the same SIR constraint for all the downlink data traffic flows in all the cells, the intercell fairness under nonuniform traffic may be achieved by constraining the power allocation per cell, i.e., $P_{B,j}$ as follows:

$$P_{B,j} \leq \left[\frac{g_j}{\frac{1}{J+1} \sum_{j=0}^J g_j} \right] P_B \quad (20)$$

for $j = 0, 1, \dots, J$.

The joint rate and power allocation for nonuniform traffic distribution can be performed after the optimal global power allocations $\{P_{B,j} \mid j = 0, 1, \dots, J\}$ have been determined by the network controller. For the suboptimal joint rate and power allocation, the per-cell power allocations $\{P_{B,j}\}$ are assumed to be given by (20).

Based on $\{P_{B,j}\}$ and $\eta_{j'/j}(k)$, the effective interference factors $\mu_k^{(j)}$, $k = 1, \dots, g_j$, can be measured and hence the rate allocations can be performed by the same algorithms used in the case of uniform traffic distribution. In this case, P_B in (15) would be replaced by $P_{B,j}$ and α_j (for *Algorithm-2*) would be given by

$$\alpha_j = \frac{N}{g_j} \left(1 - \frac{P_c}{P_{B,j}} \right) (\text{SIR})_o^{-1}. \quad (21)$$

Using ρ_j in (13) and $\{\mu_k^{(j)}\}$, the per-user power allocation at basic rate in (16) is performed to have the same downlink quality for all the MSs.

V. ANALYSIS OF SUM-RATE CAPACITY

For multicell and multirate WCDMA downlink, if uniform traffic distribution is assumed, then the achievable maximum sum-rate capacity can be estimated by taking into account the intercell interference caused by J other cells. The sum-rate capacity here refers to the average number of radio link level frames transmitted per adaptation interval to all the mobiles in a cell (i.e., $\sum_{k=1}^G m_k^{(j)}$) for which the required SIR is achieved. When the sum-rate capacity is averaged over the number of mobiles, the average-rate capacity per mobile per adaptation interval is obtained. For nonuniform traffic scenario, the average sum-rate capacity in a multicell system can be obtained based on the sum-rate capacity determined for each cell.

Since in the case of *Algorithm-1* the rate and power allocation is nonuniform with respect to the effective interference factors $\{\mu_k^{(j)}\}$, deriving closed-form theoretical results for the sum-rate capacity in this case seems to be mathematically intractable. Therefore, the sum-rate capacity in this case is analyzed by simulation. In the case of a rate and power allocation by using *Algorithm-2*, the approximate sum-rate capacity \tilde{C}_d can be investigated analytically.

A. Uniform Traffic

The sum-rate capacity in this case is given by

$$\tilde{C}_d = G \cdot \mathbf{E} \left\{ \tilde{m}_k^{(j)} \right\} \quad (22)$$

for the case with noninteger rate $\tilde{m}_k^{(j)}$ in *step (i)* of *Algorithm-2*. From *step (i)* of *Algorithm-2*, we have

$$\mathbf{E} \left\{ \tilde{m}_k^{(j)} \right\} = \alpha \cdot \mathbf{E} \left\{ \frac{1}{\mu_k^{(j)}} \right\}. \quad (23)$$

If we consider only the path loss to simplify the derivation, then the factor $L_{j'}(j, k)$ in (1) reduces to $L_{j'}(j, k) = r_{k,j'}^{-\delta}$ and $\zeta_k^{(j')} = 1$ (no fading) in which case we derive (24) below

$$\sum_{j' \neq j} \eta_{j'/j}(k) = \sum_{\substack{(k,l) \\ k+l=2n}} \left[\frac{u^2 + v^2}{\left(\frac{u \pm \sqrt{3}k}{2} \right)^2 + \left(\frac{v \pm 3l}{2} \right)^2} \right]^{\delta/2} \quad (24)$$

for a positive integer n .

Here, we assume the hexagonal cell layout with the normalized cell radius of unity and uniform distribution of mobiles in tagged cell $j = 0$. Then, the expectation $\mathbf{E} \left\{ 1/\mu_k^{(j)} \right\}$ can be derived as in (25) below

$$\begin{aligned} \mathbf{E} \left\{ \frac{1}{\mu_k^{(j)}} \right\} &= \int_0^{\sqrt{3}/2} \int_0^{u/\sqrt{3}} [(1 - \nu \\ &+ \sum_{\substack{(k,l) \\ k+l=2n}} \left(\frac{u^2 + v^2}{\left(\frac{u \pm \sqrt{3}k}{2} \right)^2 + \left(\frac{v \pm 3l}{2} \right)^2} \right)^{\delta/2}]^{-1} \\ &\times dudv \left(\frac{8}{\sqrt{3}} \right). \end{aligned} \quad (25)$$

Now, combining α in *step (i)* of *Algorithm-2* and (23) with (22), we obtain

$$\tilde{C}_d = N \left(1 - \frac{P_c}{P_B} \right) (\text{SIR})_o^{-1} \mathbf{E} \left\{ \frac{1}{\mu_k^{(j)}} \right\}. \quad (26)$$

Thus, using the two-dimensional (2-D) spatial integral in (25), the sum-rate capacity \tilde{C}_d can be numerically evaluated for varying δ .

For more realistic channels, we need to consider both the path loss and the shadowing as modeled by $L_{j'}(j, k)$ in (1) and $\zeta_k^{(j')} = 1$ (no fading) in which case $\mathbf{E}\{\mu_k^{(j)}\}$ is given by (27) below²

$$\mathbf{E}\{\mu_k^{(j)}\} \cong \int_0^{\sqrt{3}/2} \int_0^{u/\sqrt{3}} \left[(1 - \nu) + \sum_{\substack{(k,l) \\ k+l=2n}} f(k, l) \right. \\ \left. \times \left(\frac{u^2 + v^2}{\left(\frac{u \pm \sqrt{3}k}{2}\right)^2 + \left(\frac{v \pm 3l}{2}\right)^2} \right)^{\delta/2} \right] dudv \left(\frac{8}{\sqrt{3}} \right). \quad (27)$$

Similarly, as in [13], $f(k, l)$ can be evaluated as in (28) below

$$f(k, l) = \exp \left[\left(\frac{\sigma \ln 10}{10} \right)^2 \right] \left\{ 1 - Q \left[\frac{5\delta}{\sqrt{2}\sigma^2} \log_{10} \right. \right. \\ \left. \left. \times \left(\frac{\left(\frac{u \pm \sqrt{3}k}{2}\right)^2 + \left(\frac{v \pm 3l}{2}\right)^2}{u^2 + v^2} \right) - \sqrt{2}\sigma^2 \frac{\ln 10}{10} \right] \right\} \quad (28)$$

where σ is the standard deviation of the log-normal random variable ξ_j in (1), and $Q(x) = 1/\sqrt{2\pi} \int_x^\infty e^{-y^2/2} dy$. Since $\mathbf{E}\{1/\mu_k^{(j)}\} \cong 1/\mathbf{E}\{\mu_k^{(j)}\}$ (by using Jensen's inequality [18]), an approximation for the sum-rate capacity \tilde{C}_d in (26) can be obtained based on (27) and (28).

On the other hand, when $\{m_k^{(j)}\}$ is an integer in the set $\{0, 1, \dots, \varphi\}$ (as defined in *step (i)* of *Algorithm-2*), the sum-rate capacity C_d can be expressed as in (29) below

$$C_d = G \cdot \mathbf{E}\{m_k^{(j)}\} \\ \cong G \cdot \left\{ \sum_{m=1}^{\varphi-1} m \Pr \left[m - 0.5 \leq \tilde{m}_k^{(j)} < m + 0.5 \right] \right. \\ \left. + \varphi \Pr \left[\tilde{m}_k^{(j)} \geq \varphi - 0.5 \right] \right\}. \quad (29)$$

With this rate truncation, the possibility of $(\text{SIR})_{o,d} < (\text{SIR})_o$ exists, but the second-order effect is ignored here to simplify the analysis.

B. Nonuniform Traffic

The sum-rate capacity $\tilde{C}_d^{(j)}$ in cell j is similarly obtained based on $\mu_k^{(j)}$ in (10). Here, the power ratio $\beta_{j'/j}$ acts as the weighting factor and affects the level of interference from $(\text{BS})_{j'}$ to the k th mobile in cell j . The weighting effect is similar to the well-known "near-far effect," that is, the

stronger $(\text{BS})_{j'}$ produces higher intercell interference. In (25), $\mathbf{E}\{1/\mu_k^{(j)}\}$ includes the weights $\{\beta_{j'/j}\}$, and then the sum-rate capacity $\tilde{C}_d^{(j)}$ is given by (26) with $P_{B,j}$.

Considering both the path loss and the shadowing, $\mathbf{E}\{\mu_k^{(j)}\}$ can be determined using (27) when $f(k, l)$ is replaced by $f(k, l)\beta_{(k,l)/j}$ with $\beta_{(k,l)/j} = P_{B,(k,l)}/P_{B,j}$, $(k, l) \equiv j' \neq j$. Using $\mathbf{E}\{1/\mu_k^{(j)}\} \cong 1/\mathbf{E}\{\mu_k^{(j)}\}$, the sum-rate capacity $\tilde{C}_d^{(j)}$ results. To compare with the uniform traffic case, the average sum-rate capacity \tilde{C}_d per cell is evaluated as

$$\tilde{C}_d = \frac{1}{(J+1)} \sum_{j=0}^J \tilde{C}_d^{(j)}. \quad (30)$$

In the case of integer rate allocation, the sum-rate capacity $C_d^{(j)}$ is obtained similarly as in (29) where $\tilde{m}_k^{(j)} = \alpha_j/\mu_k^{(j)}$. To derive the probability distribution on $\tilde{m}_k^{(j)}$, Monte Carlo simulation is performed for $j = 0, 1, \dots, J$.

VI. SIMULATION MODEL, RESULTS AND DISCUSSIONS

A. Models for Micromobility, Shadowing, and Multipath Fading

We consider two micromobility models; the *random mobility* model and the *directional mobility* model. In the former case, the location of each mobile user during each frame time is chosen randomly inside the target cell and the effect of shadowing at different locations is assumed to be uncorrelated. In the later case, we assume a directional random walk model [15] where the mobile users travel from a starting point to a destination in a series of statistically independent discrete steps and in this case the effect of shadowing at the different locations is assumed to be correlated. For each step, the angular deviation (θ) of the travel direction from the *principal direction*³ has the probability density function $f(\theta)$ given by

$$f(\theta) = \begin{cases} \frac{A_\theta}{2[1+A_\theta^2\theta^2] \tan^{-1}(A_\theta\theta)}, & -\pi \leq \theta \leq \pi \\ 0, & \text{otherwise.} \end{cases} \quad (31)$$

The parameter A_θ controls how close the travel direction is to the principal direction. If a mobile user travels in a forward direction with probability 0.95, the corresponding value for A_θ is 4.2 [15]. We assume that all the mobile users have a constant speed of v and that for each user the successive points are separated (in time) by one frame time.

The correlated shadowing is modeled as a Gaussian white noise process, filtered through a first degree low-pass filter as follows [16]:

$$\omega_{k+1(\text{dB})} = a \times \omega_{k(\text{dB})} + (1 - a) \times v_k \quad (32)$$

where $\omega_{k(\text{dB})}$ is the mean envelope level or mean square-envelope level (in *decibels*) that is experienced at location k , a is the correlation coefficient given by $a = \varepsilon_D^{vT_s/D}$, and v_k is a zero-mean Gaussian random variable with variance $\tilde{\sigma}^2$.

Here, $\tilde{\sigma}^2 = (1 + a/1 - a)\sigma^2$, with σ^2 being the variance of log-normal shadowing. The parameter ε_D is the correlation

²The possibility of $(\text{BS})_{j'}$ ($j' \neq j$) being selected as a serving BS is ignored and, hence, this holds as an upper bound [13].

³At any point on the travel path, the line joining the point to the destination defines the principal direction.

between two points separated by distance D and T_s is the sampling interval (which is assumed to be equal to the frame-time T in this paper).

Multipath fading is assumed to be independently varying. In the random mobility case, an L -path ($L = 3$) Rayleigh fading channel with uncorrelated scattering and equal average path power is considered. Multipath fading with unequal average path power is considered for the directional mobility with correlated shadowing case and the parameters are based on the vehicular-B model [17] for macrocell.

B. Performance Metrics and Simulation Methodology

We evaluate the average transmission rate per frame-time $E(m_k^{(j)})$ for the k th mobile in cell j (i.e., *average-rate capacity*) and the *fairness in average-rate capacity* among the different mobiles (in a cell/group of cells) under the proposed joint rate and power allocation algorithms in the presence of uncorrelated shadowing and correlated shadowing for random and directional mobility model, respectively. The *average sum-rate capacity* can be obtained by multiplying the average-rate capacity obtained over *all the mobiles* (in a cell/group of cells) over the simulation period with the total number of mobiles (in a cell/group of cells).

The *intracell fairness* among $E(m_k^{(j)})$ in cell j , for $k = 1, 2, \dots, g_j$, is defined as follows:

$$F_{\text{intra}}^{(j)} = \frac{\left[\sum_{k=1}^{g_j} E(m_k^{(j)}) \right]^2}{g_j \sum_{k=1}^{g_j} E(m_k^{(j)})^2}. \quad (33)$$

The value of this fairness metric⁴ ranges from $1/g_j$ to 1.0, with 1.0 corresponding to equal average downlink transmission rate for all mobiles in cell j . The value of $1/g_j$ corresponds to the extreme case where the average downlink transmission rate for all the mobiles (except one mobile) in cell j is 0.0. intracell fairness measures the local fairness, that is, fairness among mobiles in a cell.

The *intercell fairness* among $E(m_k)$ for all mobiles in $(J+1)$ cells is defined as follows:

$$F_{\text{inter}} = \frac{\left[\sum_{j=0}^J \sum_{k=1}^{g_j} E(m_k^{(j)}) \right]^2}{\left[\left(\sum_{j=0}^J g_j \right) \sum_{j=0}^J \sum_{k=1}^{g_j} E(m_k^{(j)})^2 \right]}. \quad (34)$$

Therefore, intercell fairness measures the global fairness in the average-rate capacity.

For the random mobility with uncorrelated shadowing case, the location of the mobiles in the target cell are generated randomly during each iteration and the number of iterations used for collecting the results is sufficiently large (e.g., 10^5). In the case of directional mobility model with correlated shadowing, during each iteration, the initial locations of the mobiles are generated randomly within the target cell and the successive locations are generated by using (31) based on the mobile speed (v)

and the length of the adaptation interval (or measurement interval or frame-time T). The destination point is assumed to be located in the target cell and while generating the successive mobile locations, it is ensured that the locations are within the target cell.

It is to be noted that, the correlation between shadowing in the two successive locations is affected by the mobile speed and the measurement interval. The total number of iterations for each mobile during each simulation is taken to be sufficiently large (e.g., 10^5) to ensure reliability of the obtained performance measures.

In each case, simulations are performed to obtain the maximum average-rate capacity.⁵ For this, the intercell interference factor $\eta_{j'/j}(i)$ is calculated using (4) to evaluate the effective interference factor $\mu_i^{(j)}$ in (10). In this case, $L_j(j, i) > L_{j'}(j, i), \forall j'$ (i.e., the the BS in the “tagged cell” is selected as the serving BS). The values of $L_{j'}(j, i)$ and $L_j(j, i)$ which account for the long-term fading are assumed to be constant over a frame-time (T).

The values of $\zeta_i^{(j')}$ and $\zeta_i^{(j)}$, which account for the short-term fading in (4), are assumed to be constant only over a fraction of the frame-time Δt , where $T = K\Delta t$. Therefore, the value of $\eta_{j'/j}(i)$ over a frame time is calculated by using the average of the K independent values of $\zeta_i^{(j')}/\zeta_i^{(j)}$. The value of K is assumed to be 16 in this paper.

For all the results on *fairness* presented in this paper, the average-rate capacity (per adaptation interval) is calculated for each mobile independently by averaging over the entire simulation period. In the other cases, the average-rate capacity (per mobile per adaptation interval) is calculated by averaging over all the mobiles (in a cell/group of cells) over the entire simulation period.

To evaluate the sum-rate capacity based on (29) in the case of *Algorithm-2* (for uniform traffic load), the probability distribution of $\tilde{m}_k^{(j)}$ is obtained empirically based on the values of $1/\mu_k^{(j)}$ obtained by using Monte Carlo simulation. In this case, 10^7 values of $\mu_k^{(j)}$ are generated for randomly chosen mobile location in the center cell (cell 0) within the 3-tier cell layout (i.e., $J = 18$). Note that, if we assume $\tilde{m}_k^{(j)} = (\alpha/\mu_k^{(j)})$ as in *step (i)* of *Algorithm-2*, $\Pr[\tilde{m}_k^{(j)} < x] \equiv \Pr[1/\mu_k^{(j)} < x/\alpha]$. In the case of nonuniform traffic scenarios, the effective interference factor $\mu_k^{(j)}$ is evaluated using (10) and all the above procedures remain the same.

The values of some of the system parameters used for obtaining the results presented in this paper are listed in Table II. We consider a nonuniform traffic scenario in three cells (i.e., $J = 2$ with $g_0 = 8, g_1 = 10$, and $g_2 = 12$). The average-rate capacity per mobile ($E(m_k^{(j)})$) and the intercell fairness (F_{inter}) are calculated based on the average-rate capacity corresponding to each mobile in each of these three cells. Intracell fairness corresponding to a cell is calculated based on the average-rate capacity of the mobiles in that cell. Cell 0 is considered as the tagged cell.

⁴This is similar to the fairness function used in [19] to quantify the fairness in a shared resource system with n users: $F = ((\sum_{i=1}^n x_i)^2 / n \sum_{i=1}^n x_i^2)$ (where x_i is the i th user's throughput).

⁵The average-rate capacity may fall below this maximum value in the case of soft handoff due to increased $\eta_{j'/j}(i)$.

TABLE II
 SYSTEM PARAMETERS

$g_j, j = 0, \dots, J$	No. of mobiles in cell j
G	No. of mobiles per cell in case of uniform traffic load
$m_i^{(j)}$	Transmission rate allocated to i th mobile in cell j
$P_{b,i}^{(j)}$	Power allocated to i th mobile in cell j corresponding to the basic rate v_1
$m_i^{(j)} \times P_{b,i}^{(j)}$	Total power allocated to i th mobile in cell j
$\eta_{j'/j}(i)$	Inter-cell interference factor corresponding to transmission to i th mobile in cell j
P_c	Pilot signal transmission power
$P_{B,j}$	Total power budget available at the j th BS
P_B	Average power budget for BS transmitters per cell
β_j	Ratio of $P_{B,j}$ and P_c
$\beta_{j'/j}$	Ratio of $P_{B,j'}$ and P_B
$(SIR)_o$	Target SIR
$(SIR)_{o,d}^{(j)}$	Achieved SIR at the mobiles in cell j
$\mu_i^{(j)}$	Effective interference factor for mobile i in cell j

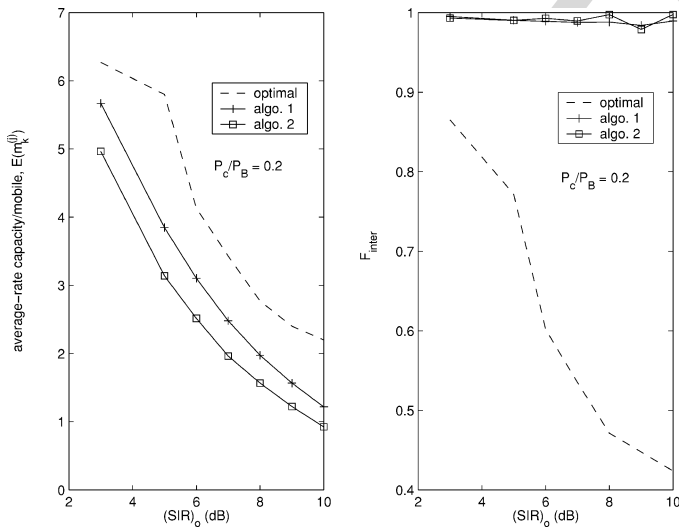


Fig. 2. Average-rate capacity per mobile and intercell fairness under different link adaptation algorithms for random mobility with uncorrelated shadowing.

C. Results and Discussions

Fig. 2 demonstrates typical variations in the average-rate capacity $E(m_k^{(j)})$ (in terms of the average number of frames transmitted per frame time per mobile) and intercell fairness (F_{inter}) with different target SIR values (i.e., $(SIR)_o$). Some typical results on the variations in $E(m_k^{(j)})$ and F_{inter} with $(SIR)_o$ are shown in Fig. 3 for the directional mobility and correlated shadowing case. As is evident from Fig. 2, the optimal

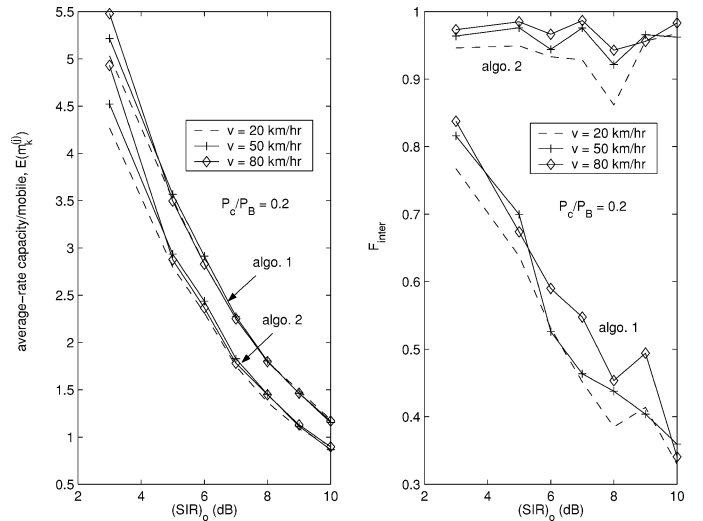


Fig. 3. Average-rate capacity (per mobile) and intercell fairness under different link adaptation algorithms for directional mobility with correlated shadowing.

rate and power adaptation algorithm provides the highest average-rate capacity (and hence the highest sum-rate capacity), but the intercell fairness deteriorates significantly.

Average-rate capacity is higher for link adaptation using *Algorithm-1* compared to that for *Algorithm-2*. In the former case, the rate allocation is primarily based on the interference experienced by a mobile and higher rates are allocated “aggressively” to the mobiles with low interference factors. In the latter case, mobiles even with high-interference factor are likely to be allocated transmission rate although it is more probable that the transmissions to these mobiles will suffer errors. Therefore, rate allocation using *Algorithm-1* results in higher average-rate capacity. As expected, $E(m_k^{(j)})$ decreases with increasing $(SIR)_o$.

The intercell and the intracell fairness in average-rate capacity for both *Algorithm-1* and *Algorithm-2* are observed to be fairly close in the case of random mobility with uncorrelated shadowing. But both the intercell and the intracell fairness improve significantly under link adaptation using *Algorithm-2* for the directional mobility with correlated shadowing case (Figs. 3 and 4). Due to more nonuniform rate allocation and at the same time correlation among the sample statistics in different locations, the rate allocation using *Algorithm-1* becomes more unfair.

Simulation results show that, for the assumed system parameters, the variation in terminal speed v (e.g., $v = 20, 50, 80$ km/hr) affects the average-rate capacity significantly only when $(SIR)_o$ is relatively small (e.g., $(SIR)_o = 3$ dB). As v increases, the value of low-pass filter gain a in (32) increases and the value of $\tilde{\sigma}^2$ decreases, and consequently, the shadowing becomes more random which tends to improve the effective interference factor. Again, when $(SIR)_o$ is reduced, γ increases [in (15)]. As a result, higher transmission rate is allocated to the mobiles, and consequently, $E(m_k^{(j)})$ increases.

Although correlated shadowing impacts the channel conditions of all the mobiles, transmission rate allocation is done

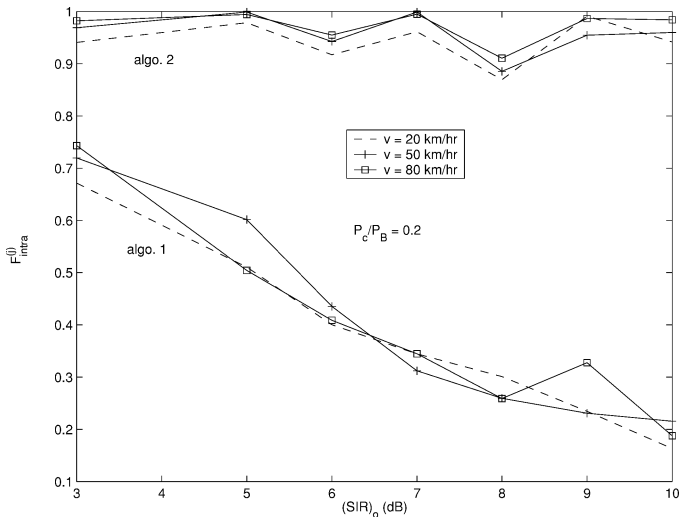


Fig. 4. Intracell fairness (in the tagged cell) under link adaptation using *Algorithm-1* and *Algorithm-2* for directional mobility with correlated shadowing.

for only a subset of the mobiles (with better channel conditions) during an adaptation interval. Again, when $(SIR)_o$ is increased, γ decreases, and consequently, the average permissible transmission rates for the mobiles decreases. These two phenomena contribute to make the impact of terminal velocity on average-rate capacity insignificant when $(SIR)_o$ is relatively high.

It is to be noted that, since power control error⁶ increases with increasing mobile speed, the average-rate capacity may deteriorate at high-user mobility conditions. The impact of imperfect power control on the dynamic rate adaptation in correlated fading channels will not be addressed in this paper.

The achieved SIR (i.e., $(SIR)_{o,d}^{(j)}$) is higher than the target SIR (i.e., $(SIR)_o$) in the case of rate allocation using *Algorithm-2*, while the achieved SIR follows the target SIR very closely in the case of rate allocation using *Algorithm-1*. This is presumably due to the lower value of $\sum_{k=1}^{G_j} m_k^{(j)} \mu_k^{(j)}$ in (9) for rate allocation using *Algorithm-2* under the constraint in (15) compared to the corresponding value in the case of *Algorithm-1*.

Typical results on the variations in $(SIR)_{o,d}$ in the tagged cell for different values of the target SIR in a nonuniform traffic scenario are presented in Fig. 5. The achieved SIR has been observed to be almost independent of the variations in other system parameters such as terminal speed and ratio of pilot-signal power to average power budget per cell (P_c/P_B).

The ratio of the control channel power to the average transmission power constraint (P_c/P_B) can be considered as a system design parameter. As P_c/P_B is reduced, the value of γ (in (15)) is increased and consequently, the average-rate capacity improves for both the rate adaptation schemes (Fig. 6). Note that, decreasing the power level of the pilot channel may make it more difficult to achieve synchronization at the mobile terminals.

It is to be noted that, the average-rate capacity in the soft handoff case would be lower than the maximum average-rate capacity. Because, in the soft handoff case (say, to cell j'),

⁶This refers to the power control to mitigate the short-term fading.

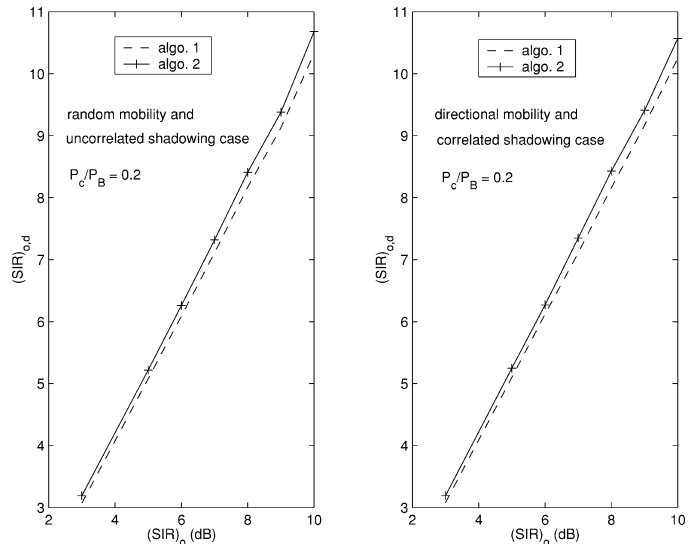


Fig. 5. Achieved SIR (in the tagged cell) under link adaptation using *Algorithm-1* and *Algorithm-2*.

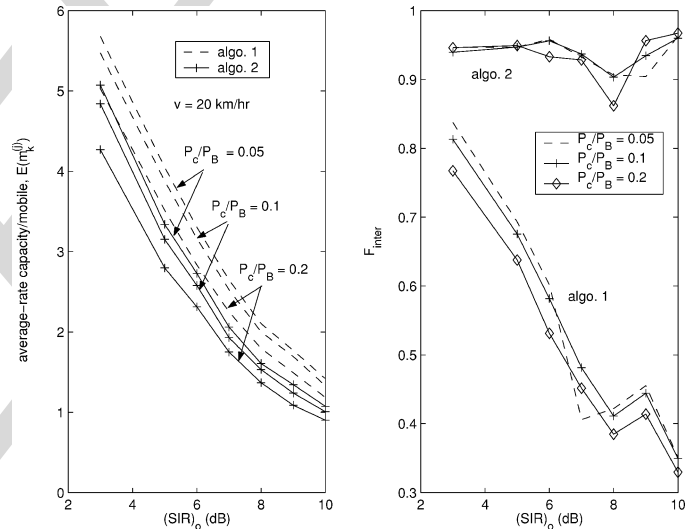


Fig. 6. Effects of variation in P_c/P_B on the average-rate capacity and intercell fairness for directional mobility with correlated shadowing.

$L_{j'}(j, i)$ is the maximum (rather than $L_j(j, i)$), which would yield higher $\eta_{j'}/j(i)$ in an average sense, and consequently, the average-rate capacity will be decreased.

The analytical results on the average-rate capacity obtained for *Algorithm-2* (for both the integer and the noninteger rates under uniform traffic load, as described in Section V) are plotted in Fig. 7 along with the simulation results for the nonuniform traffic case. In this case, the traffic load in the tagged cell is assumed to be same as the average traffic load per cell in the nonuniform case (i.e., $G = 10$). The frequency reuse factor for the mobiles in the tagged cell (cell 0) is calculated based on the interference from the other cells in a 3-tier cell layout [13] (i.e., $J = 18$ in this case).

As is observable from Fig. 7, the analytical results closely follow the simulation results. The analytical results are based on the assumption that the rate allocation is performed according to the following: $\tilde{m}_k^{(j)} = \alpha/\mu_k^{(j)}$, while the simulation results

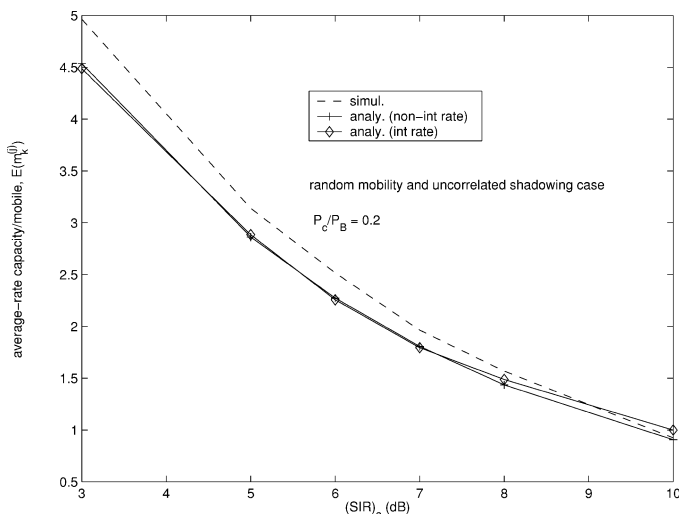


Fig. 7. Comparison between the analytical and the simulation results (for link adaptation using *Algorithm-2*, $G = 10$).

are obtained assuming that the rate allocation is performed according to the algorithm presented in Section IV. For the practical range of values of $(SIR)_o$ the analytical results well approximate the average-rate capacity under the proposed rate allocation algorithm (*Algorithm-2*). Therefore, the presented analytical methodology may be useful for system engineering and design.

VII. CONCLUSION

We analyze the SIR for downlink data transmission in cellular VSF WCDMA networks. Based upon this analysis, the solution to the optimal rate and power allocation problem (under constrained SIR and maximum transmission power at the BS) is devised. Two easy-to-implement and simple suboptimal dynamic rate and power allocation algorithms, namely, *Algorithm-1* and *Algorithm-2* are proposed. For optimal rate allocation, the transmission powers of the different BS transmitters are determined using an exhaustive search (of exponential time complexity) while for suboptimal rate allocation, the BS transmission power allocation is determined in a heuristic manner and the rate allocation algorithms have linear time complexity. Between the two interference-based dynamic rate adaptation algorithms, *Algorithm-1* is more “aggressive” and nonuniform in nature while the other entails a more uniform dynamic rate allocation.

The average-rate capacity and the intercell/intracell fairness in average-rate capacity have been analyzed under multipath fading, random mobility with uncorrelated shadowing and directional mobility with correlated shadowing. The approximate average/sum-rate capacity in the case of *Algorithm-2* has been evaluated analytically for the random mobility with uncorrelated shadowing case.

The suboptimal dynamic rate and power allocation schemes provide better intercell/intracell fairness compared to the optimal scheme, but at the cost of moderate loss in average-rate capacity. Rate adaptation using *Algorithm-1* provides higher average-rate capacity compared to that for *Algorithm-2*, but the

intercell/intracell fairness is significantly better for the latter scheme in a correlated shadow fading channel.

The SIR model along with the dynamic rate and power allocation mechanisms for downlink data transmission presented in this paper can be used to model and evaluate the performance of transport layer protocols (e.g., TCP) in wireless Internet access scenarios in cellular multirate WCDMA networks. Specifically, investigation of the impact of the transmission delay variance at the radio link level (for example, due to some aggressive dynamic rate adaptation scheme) on the end-to-end throughput performance and end-to-end throughput fairness would be of much interest. The framework for dynamic rate adaptation presented in this paper would enable us to explore the radio link level and the transport level protocol interactions in WCDMA-based cellular data networks.

ACKNOWLEDGMENT

The authors wish to thank all the reviewers for their comments and suggestions which greatly improved the presentation of this work.

REFERENCES

- [1] M. O. Sunay and J. Kahtava, “Provision of variable data rates in third generation wideband DS CDMA systems,” in *IEEE Proc. WCNC '99*, pp. 505–509.
- [2] R. V. Nobelen, N. Seshadri, J. Whitehead, and S. Timiri, “An adaptive radio link protocol with enhanced data rates for GSM evolution,” *IEEE Pers. Commun.*, vol. 6, pp. 54–64, Feb. 1999.
- [3] S. A. Jafar and A. Goldsmith, “Optimal rate and power adaptation for multirate CDMA,” in *IEEE Proc. VTC '2000 (Fall)*, 2000, pp. 994–1000.
- [4] A. Sampath, P. S. Kumar, and J. M. Holtzman, “Power control and resource management for a multimedia CDMA wireless system,” in *IEEE Proc. PIMRC '95*, 1995, pp. 21–25.
- [5] S.-J. Oh and K. M. Wasserman, “Adaptive resource allocation in power constrained CDMA mobile networks,” in *IEEE Proc. WCNC '99*, 1999, pp. 510–514.
- [6] D. Ayyagari and A. Ephremides, “Power control based admission algorithms for maximizing throughput in DS-CDMA networks with multimedia traffic,” *IEEE Proc. WCNC '99*, pp. 631–635, 1999.
- [7] S. Ulukus and L. J. Greenstein, “Throughput maximization in CDMA uplinks using adaptive spreading and power control,” in *IEEE Proc. ISSSTA '00*, Sept. 2000, pp. 565–569.
- [8] S. Ramakrishna and J. M. Holtzman, “A scheme for throughput maximization in a dual-class CDMA system,” *IEEE J. Select. Areas Commun.*, vol. 16, pp. 830–844, Aug. 1998.
- [9] A. Bedekar *et al.*, “Downlink scheduling in CDMA data networks,” in *IEEE Proc. GLOBECOM '99*, vol. 5, Nov. 1999, pp. 2653–2657.
- [10] S.-J. Oh and K. M. Wasserman, “Dynamic spreading gain control in multiservice CDMA networks,” *IEEE J. Select. Areas Commun.*, vol. 7, pp. 918–927, May 1999.
- [11] S.-J. Oh, T. L. Olsen, and K. M. Wasserman, “Distributed power control and spreading gain allocation in CDMA data networks,” in *IEEE Proc. INFOCOM '00*, vol. 2, June 2000, pp. 379–385.
- [12] E. Dahlman *et al.*, “UMTS/IMT-2000 based on wideband CDMA,” *IEEE Commun. Mag.*, vol. 36, pp. 70–80, Sept. 1998.
- [13] K. S. Gilhousen *et al.*, “On the capacity of a cellular CDMA system,” *IEEE Trans. Veh. Technol.*, vol. 4, pp. 303–312, May 1991.
- [14] V. A. Alfred and D. U. Jeffrey, *Foundations of Computer Science*, C ed. Rockville, MS: Computer Science, 1998.
- [15] K. T. Kim and C. Leung, “Generalized paging schemes for cellular communications systems,” in *IEEE Proc. PACRIM '99*, 1999, pp. 217–220.
- [16] M. Gudmundson, “Correlation model for shadow fading in mobile radio systems,” *IEE Electron. Lett.*, vol. 27, pp. 2145–2146, **Month Year**.
- [17] “Guidelines for Evaluation of Radio Transmission Technologies for IMT-2000,” ITU, Rec. ITU-R M.1225, 1997.
- [18] A. J. Viterbi, A. M. Viterbi, and E. Zehavi, “Other-cell interference in cellular power-controlled CDMA,” *IEEE Trans. Commun.*, vol. 42, pp. 1501–1504, Feb./Mar./Apr. 1994.

- [19] D. Chiu and R. Jain, "Analysis of increase and decrease algorithms for congestion avoidance in computer networks," *Computer Networks and ISDN Systems*, vol. 17, pp. 1–14, **Month Year**.



Dong In Kim (S'89–M'91–SM'02) received the B.S. and M.S. degrees in electronics engineering from Seoul National University, Seoul, Korea, in 1980 and 1984, respectively, and the M.S. and Ph.D. degrees in electrical engineering from the University of Southern California (USC), Los Angeles, in 1987 and 1990, respectively.

From 1984 to 1985, he was with the Korea Telecommunication Research Center, **Location**, as a Researcher. During 1986–1988, he was a Korean Government Graduate Fellow in the Department of Electrical Engineering, University of Southern California. From 1988 to 1990, he was a Research Assistant at the USC Communication Sciences Institute. Since 1991, he has been with the University of Seoul, Seoul, Korea, where he is currently an Associate Professor in the Department of Electrical and Computer Engineering, leading the Wireless Communications Research Group. He was a Visiting Professor at the University of Victoria, Victoria, BC, Canada, during 1999–2000. He has given many short courses and lectures on the topics of spread-spectrum and wireless communications at several companies. Since 1988, he has performed research in the areas of packet radio networks and spread-spectrum systems. His current research interests include spread-spectrum systems, cellular mobile communications, indoor wireless communications, and wireless multimedia networks.

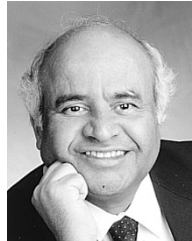
Dr. Kim has served as an Editor of the *IEEE JOURNAL ON SELECTED AREAS IN COMMUNICATIONS Wireless Communications Series* and also as a Division Editor for the *Journal of Communications and Networks*. He currently serves as an Editor for Spread-Spectrum Transmission and Access for the *IEEE TRANSACTIONS ON COMMUNICATIONS* and as an Editor for the *IEEE TRANSACTIONS ON WIRELESS COMMUNICATIONS*.



Ekram Hossain (S'98–M'01) received the B.Sc. and M.Sc. degrees in Computer Science and Engineering from Bangladesh University of Engineering and Technology (BUET), Dhaka, Bangladesh, in 1995 and 1997, respectively, and the Ph.D. in electrical engineering from the University of Victoria, Canada, in 2000.

He is working as an Assistant Professor in the Department of Electrical and Computer Engineering, University of Manitoba, Winnipeg, Canada. His main research interests include radio link control and transport layer protocol design issues for the next-generation wireless data networks.

Dr. Hossain is serving as an Editor for the *IEEE TRANSACTIONS ON WIRELESS COMMUNICATIONS*.



Vijay K. Bhargava (S'70–M'74–SM'02–F'92) received the B.Sc., M.Sc., and Ph.D. degrees from Queen's University, Kingston, Canada, in 1970, 1972, and 1974, respectively.

He is a Professor of electrical and computer engineering at the University of Victoria and is currently spending a sabbatical year at the Hong Kong University of Science and Technology, Clear Water Bay, Kowloon. He is a co-author of the book *Digital Communications By Satellite* (New York: Wiley, 1981) and co-editor of the IEEE Press Book

Reed-Solomon Codes and Their Applications. He is an Editor-in-Chief of *Wireless Personal Communication*, a Kluwer Periodical. His research interests are in multimedia wireless communications.

Dr. Bhargava is very active in the IEEE. He was the President of the IEEE Information Theory Society in 2000. He was Co-Chair for IEEE ISIT'95, Technical Program Chair for IEEE ICC'99 and is the Chair of IEEE VTC'2002 Fall. He is a Fellow of the B.C. Advanced Systems Institute, Engineering Institute of Canada (EIC) and the Royal Society of Canada. He is a recipient of the IEEE Centennial Medal (1984), IEEE Canada's McNaughton Gold Medal (1995), the IEEE Haraden Pratt Award (1999), and the IEEE Third Millennium Medal (2000).